Colloidal Stabilization by Adsorbed Gelatin

C. N. Likos, K. A. Vaynberg, H. Lwen, and N. J. Wagner

Langmuir, **2000**, 16 (9), 4100-4108• DOI: 10.1021/la991142d • Publication Date (Web): 25 March 2000

Colloidal Stabilization by Adsorbed Gelatin

C. N. Likos,*,† K. A. Vaynberg,‡ H. Löwen,† and N. J. Wagner‡

Institut für Theoretische Physik II, Heinrich-Heine-Universität Düsseldorf, Universitätsstrasse 1, D-40225 Düsseldorf, Germany, and Center for Molecular and Engineering Thermodynamics, Department of Chemical Engineering, University of Delaware, Newark, Delaware 19716

Received August 24, 1999. In Final Form: January 13, 2000

The stabilizing effect of adsorbed polyampholyte on colloidal dispersions is quantified through small angle neutron scattering measurements of the structure of concentrated dispersions. Gelatin is adsorbed onto colloidal acrylic latex particles of like net charge to provide both steric and electrostatic stabilization. The extent and structure of the adsorbed gelatin corona is measured using dynamic light scattering (DLS), small angle neutron scattering (SANS) and dilution viscometry (DV). The SANS spectra from concentrated dispersions of bare and gelatin-coated colloidal particles are modeled via integral equation theory using pair potentials that superimpose an electric double layer and a simple model of steric repulsion, where all the parameters are determined a priori. Our results demonstrate for the first time that the stabilizing forces arising from the adsorbed gelatin can be predicted quantitatively from a simple combination of Derjaguin−Landau−Verwey−Overbeek (DLVO) theory and a model for the adsorbed polymer brush. These results agree with previous studies of the surface forces of gelatin adsorbed onto mica cylinders and are important for understanding colloidal stabilization imparted by adsorbed polyampholytes.

1. Introduction

Understanding the nature of gelatin adsorption and relating it to the conformation of gelatin molecules is a problem of wide interest in food processing,[1] photography,[2] electrochemistry,[3] biology, implant medicine, and engineering. The importance of understanding protein and polypeptide adsorption and a general review of the area has been presented by Möbius and Miller.[4] Gelatin is a well-known stabilizer used in both suspensions[5] and emulsions.[6] Stabilization of the former systems is accomplished by the adsorbed gelatin acting as a steric barrier, whereas emulsions stabilization is achieved by modification of interfacial properties. This study is partly motivated by the goal of understanding gelatin stabilization of colloidal latex particles, which is technically important in controlling gelatin-containing formulations.

This work is also motivated by the complexity of polyampholyte−colloid interactions. The conformation of gelatin in solution and its adsorption onto surfaces is controlled by a delicate balance of the ampholytic nature of the polypeptide, polymer character, hydrophobic forces, and polydispersity. Consequently, numerous variables can be expected to affect the adsorbed amount and the structure of the adsorbed layer, such as, temperature, ionic strength, pH, gelatin molecular weight and distribution, surface chemistry, solvent quality, and possibly surface geometry. Some recent experimental investigations of gelatin adsorption onto model colloidal particles provide a review of the field to date.[7,8]

Several methods have been used to study the stabilizing effects resulting from gelatin adsorption.[9] Most relevant for the work performed here are the direct measurements of the forces between layers of gelatin adsorbed on mica cylinders through the use of the surface forces apparatus (SFA). Kawanishi et al.[10] explored the force between layers of gelatin adsorbed to mica surfaces both above and below its isoelectric point (pH = 5.1) using a SFA. The adsorbed amount of gelatin was calculated from the mean refractive index of the medium between the mica sheets. The authors reported a dependence of the adsorbed amount and the range of the layer interactions on the pH and ionic strength of the solutions. The measured force vs distance curves were fit with a linearized, constant-potential electrostatic interaction.[11]

Kamiyama and Israelachvili[12] performed adsorption and SFA measurements on gelatin adsorbed onto mica from aqueous NaCl solutions. Particular attention was paid to the effect of ionic strength and pH on the excess adsorbed gelatin and on the force between the plates as a function of their separation. They found that the amount of added salt has a marginal effect on the adsorption properties, but a rather pronounced effect on the force between the plates: for high salt concentrations, the force is dominated by the steric effects, that is, the compression energy between two overlapping gelatin layers, which is very well described by the Alexander-de Gennes equation.[13,14] On the other hand, if the salt concentration is low, the electrostatic double-layer repulsion between the plates is not screened and the forces display long-range tails quantifiable via an electrostatic repulsion.[11]

† Heinrich-Heine-Universität Düsseldorf.

‡ University of Delaware.

(1) Ward, A. G.; Courts, A. In *The Science and Technology of Gelatin*; Academic Press: London, 1977.

(2) Mees, K. C. E. In *The Theory of Photographic Process*; Macmillan: New York, 1966.

(3) Brown, G. M.; Hope, G. A. *J. Electroanal. Chem.*, **1995**, *397*, 293.

(4) Möbius, D., Miller, R., Eds. *Proteins at Liquid Interfaces*; Elsevier: Amsterdam, 1998.

(5) Maternaghan, T. J.; Banghan, O. B.; Ottewill, R. H. *J. Photogr. Sci.* **1980**, *28*, 1.

(6) Rodin, V. V.; Izmailova, V. N. *Colloids Surf.*, **1996**, *106*, 95.

(7) Vaynberg, K. A.; Wagner, N. J.; Sharma, R.; Martic, P. *J. Colloid Interface Sci.*, **1998**, *205*, 131.

(8) Cosgrove, T.; Hone, J. H. E.; Howe, A. M.; Heenan, R. K. *Langmuir* **1998**, *14*, 5376−5382.

(9) Braithwaite, G. J. C.; Luckham, P. F.; Howe, A. M. *J. Colloid Interface Sci.* **1999**, *213*, 525−545.

(10) Kawanishi, N.; Christenson, H. K.; Ninham, B. W. *J. Phys. Chem.* **1990**, *94*, 4611.

(11) Hunter, R. J. *Foundations of Colloid Science*, Clarendon Press: Oxford, 1987; Vol. I.

(12) Kamiyama, Y.; Israelachvili, J. *Macromolecules* **1992**, *25*, 5081.

(13) Alexander, S. *J. Phys.* (*Les Ulis, Fr.*) **1977**, *38*, 983.

(14) de Gennes, P. G. *C. R. Acad. Sci. Ser. II, Fascicule B Mechanique Physique Chimie Astronomie* **1985**, *300*, 839.

10.1021/la991142d CCC: $19.00
Published on Web 03/25/2000

Because of recently reported molecular scale measurements of the structure and amount of gelatin adsorbed onto model surfaces using X-ray reflectometry[15] and neutron reflectometry,[16] it is now possible to provide a detailed molecular-level description of polyampholyte adsorption onto macroscopic surfaces and the consequent colloidal forces. Other methods have been attempted to quantify the forces acting between more microscopic surfaces, such as the rheology measurements of Howe et al.[17] They characterized the viscosity of oil in water emulsions stabilized with gelatin and used a phenomenological model to extract pair potentials. Although the results for the stabilizing force due to adsorbed gelatin were within the realm of expectation, the method relied on phenomenological modeling and hence it was not predictive. To date, no method has been proposed to predict quantitatively the interparticle potential resulting from adsorbed gelatin.

Questions remain regarding the adsorption properties of gelatin onto highly curved surfaces, such as afforded by colloidal latex particles, and the resultant interaction between two such coated particles. Recently, it has been demonstrated that accurate measurements of the structure of gelatin adsorbed on colloidal particles can be achieved through a combination of methods that includes dynamic light scattering, small angle neutron scattering, (SANS), viscometry, densitometry, and solution depletion with fluorescent labeled gelatin.[7,8] In this article, we investigate the consequence of gelatin adsorption onto well-characterized, model, spherical polymer colloids by resolving the dispersion structure factor over a range of concentrations. Statistical mechanics provides a rigorous link between the structure of a colloidal dispersion as measured by scattering methods and the direct interaction potential between the particles.[18] SANS measurements are performed on concentrated solutions of bare and gelatin-coated latex particles and compared with integral equation theory, which provides an exact method for predicting scattering spectra[18−20] based on parameters determined from independent measurements. We demonstrate that a simple superposition of interaction potentials for electrostatic repulsion and polymer brush steric forces suffices to predict the observed scattering data, in agreement with expectations from the measurements surface forces.

This article is organized as follows. In the next section we describe the experimental methods and the theoretical methods required to predict the dispersion structure. After that we present and discuss the results of the SANS measurements. Then we compare the predictions and measurements and draw conclusions from analysis of the results.

2. Experimental Section

Materials. Acrylic-based latex [dynamic light scattering (DLS) radii of 330 ± 30 Å and 450 ± 40 Å] and lime-processed, deionized bone gelatin (M_n = 100 000, M_w = 160 000, Bloom: 295 g at 6.7% w/v gel at 10 °C, isoelectric point at pH = 5.1) were provided by Eastman Kodak Company and have been investigated previously.[7] Hydrodynamic sizes were determined from velocity auto correlation functions (VACF) obtained on a 164-channel BI-9000AT digital correlator using 488-nm laser light scattered from diluted (∼0.03% weight fraction) dispersions. The single particle diffusivity was extracted from a second-order cummulant analysis of the auto correlation function and hydrodynamic radius (R_h) of the particles is calculated by the Stokes−Einstein equation. Polydispersity was determined from the ratio of second to first cumulant. Note that the neutron scattering length density of latex was determined previously by contrast variation[7] to be 6.9 × 10^9 cm^{-2}.

The SANS experiments were performed on the NG3 SANS line at the National Institute of Standards and Technology (NIST) in Gaithersburg, MD, using 1-mm-thick banjo cells at 40 °C. Thermal neutrons of 6 Å and 14.7% full width at half-maximum (fwhm) were used at detector distances of 5 and 13 m, resulting in a momentum transfer between 0.0047 and 0.0945 $Å^{-1}$. All solutions were prepared in 10 mM pH 5.7 sodium acetate buffer made with either H_2O or D_2O, depending on the nature of the experiment. In the experiments involving adsorbed gelatin, colloidal latex gelatin mixtures were incubated at 40 °C for 8−10 h. The samples used in shell contrast experiments were equilibrated, centrifuged, and then re-suspended in clear, contrast matching aqueous buffer.

The collected SANS data are reduced according to the standard procedures recommended by NIST. Corrections for the empty cell, detector efficiency, and sample transmission are applied with software provided by NIST. The data are placed on an absolute scale by ratioing with scattering obtained by NIST calibrated standards. Finally, the data are angle-averaged and Porod plots ($I * Q^4$ vs Q^4) generated to determine the incoherent background scattering. The spectra reported here have had the incoherent background removed. However, no deconvolution of the instrument "smearing" function has been performed, because we prefer to smear the theoretical predictions with the known instrument smearing function for direct comparison with the data.

The cited electrophoretic mobility was determined by use of a Brookhaven ZetaPlus over a range of pH and added salt values encompassing those of the SANS measurements. Experimental procedures for the remainder of the cited data have been published by Vaynberg et al.[7]

3. Theoretical Predictions of the SANS Scattering from Gelatin-stabilized Colloidal Particles

In this section we present the method of generating the theoretical predictions that will be compared with the SANS measurements of both dilute and concentrated solutions of bare (electrostatically stabilized) and gelatin-coated latex particles. At low concentrations, the correlations between different particles are very weak and can be ignored; the scattering intensities result from scattering from a single particle and they allow us to determine important parameters such as the particle size and the extent of the adsorbed gelatin layer ("corona"). These parameters are necessary for the theoretical predictions of the scattering at higher concentrations where correlations between particles become important.

Neglecting interparticle scattering contributions, the coherent macroscopic scattering intensity of a SANS experiment $I(Q)$ is given by the expression[18,21,22]:

$$I_{th}(Q) = \frac{N_z}{V}\langle |A(Q)|^2 \rangle \quad (1)$$

Here, Q is the scattering vector which is given by 4π sin-

(15) Vaynberg, K. A.; Wagner N. J.; Ahrens, J.; Helm, C. A. *Langmuir* **1999**, *15*, 4685−4689.
(16) Turner, S. F.; Clarke, S. M.; Rennie, A.; Thirtle, P. N.; Li, Z. X.; Thomas, R. K.; Langridge, S.; Penfold, J. *Prog. Colloid Polymer Sci.*, submitted for publication, 1999.
(17) Howe, A. M.; Clarke, A.; Whitesides, T. H. *Langmuir* **1997**, *13*, 2617.
(18) Wagner, N. J.; Krause, R.; Rennie, A.; D'Aguanno, B. *J. Chem. Phys.* **1991**, *95*, 494.
(19) Rogers, F. A.; Young, D. A. *Phys. Rev. A* **1984**, *30*, 999.
(20) Bergenholtz, J.; Wagner, N. J.; D'Aguanno, B. *Phys. Rev. E* **1996**, *53*, 2968.
(21) Poppe, A.; Willner, L.; Allgaier, J.; Stellbrink, J.; Richter, D. *Macromolecules* **1997**, *30*, 7462.
(22) Higgins, J. A.; Benot, H. C. *Polymers and Neutron Scattering*; Oxford Science Publications, Clarendon Press: Oxford, 1994.

$(\theta/2)/\lambda$, where θ is the scattering angle and λ is the neutron wavelength. Moreover, N_z is the number of scatterers in the volume V, and $A(Q)$ is the scattering amplitude from a single particle. In the expression above it is assumed that the incoherent background scattering has been subtracted off and no instrument smearing is present.

The subscript on the left-hand side of eq 1 denotes the fact that the scattering intensity given by this equation is, at this stage, still a theoretical quantity; to have a direct comparison with experimental data, the finite resolution of the experimental apparatus has to be taken into account (i.e., instrument "smearing"). This is achieved by making a convolution of the quantity $I_{th}(Q)$ with the resolution function $R(Q,Q_0)$[23] as:

$$I(Q) = \int_0^\infty dQ_0 I_{th}(Q_0) R(Q,Q_0) \tag{2}$$

For the instrument NG3 at NIST, the resolution function is modeled as triangular with the given mean and fwhm. The quantity $I(Q)$ is then directly comparable with absoluted SANS data with the incoherent background subtracted off.

For spherical scatterers having a core−shell structure, the scattering amplitude $A_{C,Sh}$ can be written as follows:

$$A_{C,Sh}(Q) = (\rho_{Sh} - \rho_S)F(Q; R_M) + (\rho_C - \rho_{Sh})F(Q; R_C) \tag{3}$$

where $F(Q; R_M)$ and $F(Q; R_C)$ are the form factors of the coated particle, which have radius R_M, and of the core, which has radius R_C, respectively. Moreover, ρ_C, ρ_{Sh}, and ρ_S are the scattering length densities of the core, the shell, and the solvent, respectively, The scattering length density ρ_i of the component i in the mixture is calculated as

$$\rho_i = \frac{\sum_z b_z}{v_i} \tag{4}$$

where b_z is the coherent scattering length of an atom z in the solvent or of a repeat unit in a polymeric molecule and v_i is the respective volume; the sum is carried, hence, over all atoms in a molecule or in the repeat unit.

The scattering length density of aqueous solvents can be varied by substituting heavy water, that is, D_2O for water. The scattering length density of a H_2O/D_2O mixture is given as:

$$\rho_S = \phi_{H_2O}\rho_{H_2O} + (1 - \phi_{H_2O})\rho_{D_2O} \tag{5}$$

with ϕ_{H_2O} denoting the volume fraction of H_2O in the isotopic water mixture. $\rho_{H_2O} = -0.562 \times 10^{10}$ cm^{-2} and $\rho_{D_2O} = 6.404 \times 10^{10}$ cm^{-2} denote the scattering length densities of the pure solvents. In this way, one can fulfill either the condition $\rho_{Sh} = \rho_S$ or the condition $\rho_C = \rho_S$. The first case is denoted as core contrast and the second as shell contrast. The dilute limiting scattering results for core contrast are identical with the case of bare (uncoated) particles. Shell contrast provides a method to determine the extent of the gelatin layer. We examine the cases of core and shell contrast in more detail below.

3.1. Core Contrast or Bare Particles. In this case, where shell and solvent scatter neutrons in the same way, only the core is visible and eq 3 takes the form:

$$A_{C,Sh}(Q) = (\rho_C - \rho_S)F(Q; R_C) \tag{6}$$

Combining eqs 1 and 6, we obtain for the scattering intensity the expression:

$$I_{th}(Q) = n_C(\rho_C - \rho_S)^2 F^2(Q; R_C) \tag{7}$$

where n_C is the number density of the colloidal particles.

For spherical particles having radius R_C and volume $V_C = 4\pi R_C^3/3$, the form factor $F(Q; R_C)$ is analytically known in theRayleigh−Gans−Debye limit[24]:

$$F(Q; R_C) = 3V_C \frac{\sin(QR_C) - QR_C\cos(QR_C)}{(QR_C)^3} \tag{8}$$

Using eqs 2, 7, and 8 above, we can determine the size of the bare latex particles by fitting the intensity data at low concentration and using the radius R_C of the particles as the only free parameter, where the scattering length density of the particles is either calculated from the known structure and density, or determined independently from contrast matching experiments.

3.2. Shell Contrast. In this case, where the solvent and the core scatter neutrons in the same way and only the corona is visible, we obtain from eq 3:

$$A_{C,Sh}(Q) = (\rho_{Sh} - \rho_C)[F(Q; R_M) - F(Q; R_C)] \tag{9}$$

Hence, the total scattering intensity is now given by the expression:

$$I_{th}(Q) = n_C(\rho_{Sh} - \rho_C)^2[F(Q; R_M) - F(Q; R_C)]^2 \tag{10}$$

Once again, we obtain a comparison with SANS data by means of convolution of $I_{th}(Q)$ with the resolution function. The form factor $F(Q; R_M)$ is given by eq 8 above, after replacing R_C by R_M and V_C by V_M.

Once the bare particle radius has been determined, for example, by the method outlined in section 3.1, the shell contrast procedure can be applied to low-concentration solutions using now R_M as the only free parameter to obtain the thickness $L = R_M - R_C$ of the adsorbed layer. Note that this analysis is based on the assumption, as in previous work,[7] that the gelatin density is uniform in the corona. Further, as our focus is on structural effects that are manifest at lower scattering vectors, to be discussed next, in this and in the preceding section we have neglected any effects of fluctuations in the adsorbed layer, an effect that has been treated in depth in ref 8. Finally, the adsorbed amount, which is measured independently via solution depletion and fluorescence labeling (see ref 7), can be determined in principle from a Guinier analysis (see, e.g., ref 8); however, the range of scattering vectors probed here and the size of the corona precludes an accurate determination of the adsorbed amount directly from SANS.

3.3. Scattering from Concentrated Dispersions. When the concentration of the colloidal particles in the solution increases, spatial correlations between the colloids become evident in the scattering patterns. Because the total scattering intensity obtained in a SANS experiment is strongly influenced by the interactions between the particles and the measured SANS profiles, and these correlations can be traced directly to the effective pair potential between the scatterers, SANS provides a method to resolve pair interaction potentials directly in concentrated dispersions.

(23) Ramakrishnan, K. *J. Appl. Crystallogr.* **1985**, *18*, 42.

(24) See, e.g., Glatter, O.; Kratky, O. *Small-Angle X-ray Scattering*; Academic Press: London, 1982.

The starting point of a theoretical approach[25,26] to the problem is to assume a pairwise additive interaction potential between the particles, which we denote by $V(r)$, r being the separation between the particle centers. In the modern theory of the liquid state,[27] a large variety of so-called integral equation theories have been developed, which allow for the evaluation of the radial distribution function $g(r; n)$ of a dense liquid having number density n, once the pair potential is known. The radial distribution function is proportional to the probability of finding a particle in the liquid at a distance r from a given, reference particle, taken to be located at the origin. Associated with the radial distribution function is the total correlation function $h(r) = g(r) - 1$, the Fourier transform of which yields the structure factor $S(Q)$ as

$$S(Q) = 1 + n \int d\mathbf{r} \exp[-i\mathbf{Q}\cdot\mathbf{r}]h(\mathbf{r}) \qquad (11)$$

For atomic liquids, it has long been known that the structure factor establishes a bridge between theory and experiment. For such liquids the form factor is just the square of the volume of the scatterer and so the scattering intensity yields $S(Q)$ directly. For a colloidal suspension, whose constituent entities are large particles, the form factor of the individual particles has to be considered.[25,28] Furthermore, the complication of size, shape, and scattering length density polydispersity must be considered.[18,26] In this work, because our particles are nearly monodisperse, we can ignore polydispersity effects and treat the scattering from monodisperse dispersions. For a concentrated, monodisperse dispersion, eq 1 becomes:

$$I_{th}(Q) = \frac{N_z}{V}\langle|A(Q)|^2\rangle S(Q) \qquad (12)$$

where it is evident that the structure factor $S(Q)$ becomes uncoupled from the determination of the form factor. The effects of paucidispersity[25,29] and finite size polydispersity[26,28] on the scattering are well documented, but will not be included here. The primary effect of polydispersity in the range of scattering vectors considered here is to "smear" the minima in the form factor, as seen in the comparisons that follow.

Three factors permit this simplification for our system. First, the colloids are nearly monodisperse, because the polydispersity is less than 7%, as determined by photon correlation spectroscopy. Second, the presence of instrument smearing tends to mask small amounts of polydispersity, making it impossible to resolve polydispersities of this magnitude by SANS. Finally, our comparison with theory is for wavevectors around or greater than the first maximum, whereas the most significant effect of paucidispersity is for wavevectors much lower than the primary peak in the structure factor.

For the concentrated dispersions, no contrast matching was performed and the form factor is taken to be that of the measured, dilute colloidal particle. Because the adsorbed mass of gelatin is very small in relation to the mass of the colloidal particle (<1% weight fraction), the contribution of the gelatin corona to the form factor scattering is negligible away from core contrast matching. Hence, we determined it is sufficiently accurate to use the same form factor for all the scattering predictions of the concentrated dispersions. Thus, for both bare and coated particles, the theoretical scattering intensity is given by the equation:

$$I_{th}(Q) = n_C(\rho_C - \rho_S)^2 F^2(Q; R_C)S(Q) = \qquad (13)$$

$$= I_0\left(3\frac{\sin(QR_C) - QR_C\cos(QR_C)}{(QR_C)^3}\right)^2 S(Q) \qquad (14)$$

where we have defined the prefactor I_0, which depends only on the density of the sample, the scattering length densities of the colloids and the solvent, and the size of the colloidal particle:

$$I_0 = n_C(\rho_C - \rho_S)^2 V_C^{\,2} \qquad (15)$$

Differences in scattering between the bare and coated particles at equal concentration can be traced directly back to a difference in the pair interaction potential, which affects the structure factor $S(Q)$. Again, to have a direct comparison with experimental data, the above-obtained theoretical intensity $I_{th}(Q)$ must be convoluted with the resolution function of the experimental apparatus, (see eq 2). We now propose interaction potentials suitable for describing the bare and gelatin-coated latex particles.

3.4. Bare Particle Interaction Potential. The acrylic latex particles used in this study are negatively charged and are suspended in a sodium acetate buffer of 10 mM. For the purpose of calculation, we estimate the number of surface charges Z from the measured value of the zeta potential (−77 mV), which we take to be the surface potential ψ_0 and the following relationship[11]:

$$\psi_0 = \frac{Ze}{4\pi\epsilon_0\epsilon_r R_C(1 + \kappa R_C)} \qquad (16)$$

In eq 16, $\epsilon_0 = 8.84 \times 10^{-12}$ (SI) is the dielectric constant of vacuum, ϵ_r is the dielectric constant of the solvent ($\epsilon_r = 81$ for water), k_B is Boltzmann's constant, and T is the absolute temperature. The inverse Debye length κ gives the electrostatic screening length and is given by[11]:

$$\kappa = |e|\sqrt{\frac{\sum_i n_i z_i^2}{\epsilon_0\epsilon_r k_B T}} \qquad (17)$$

The sum is carried over all ionic species present in the solution except for the colloidal particles themselves; n_i and z_i are the solution phase concentration and charge of the ith species. Using the known value of the colloid radius R_C and eq 17 with $n_C \to 0$ and eq 16, we obtain the value $Z = 1227$ for the surface charge of the latex particles having hydrodynamic radius $R_h = 330$ Å.

It is generally accepted that the Derjaguin−Landau−Verwey−Overbeek (DLVO) theory of charged interfaces accurately describes the effective interaction between charged colloids in an ionic environment.[11] For these values of ionic strength, surface charge, and particle size we neglect the attractive influence of London−van der Waals forces. The functional form of the electrostatic interaction depends on the value of the dimensionless parameter κR_C. For small values of κR_C, a Yukawa form is suitable. In Table 1 we present the values of κR_C for the four mixtures we studied. The high concentration of salt present in the

(25) Hayter, J. B. In *Physics of Amphiphiles: Micelles, Vesicles, and Microemulsions, Proceedings of the International School of Physics 'Enrico Fermi'*; North-Holland: Amsterdam, 1985.

(26) D'Aguanno, B.; Klein, R. *J. Chem. Soc., Faraday Trans.* **1991**, *87*, 379.

(27) See, e.g., Hansen, J. P.; McDonald, I. R. *Theory of Simple Liquids*, 2nd ed.; Academic Press: London, 1986.

(28) Kaler, E. W. In Brumberger, H., Ed.; *Modern Aspects of Small-Angle Scattering*; Kluwer Academic: Dordrecht, 1995; pp 329−353.

(29) Kotlarchyk, M.; Chen, S.-H.; Huang, J. S.; Kim, M. W. *Phys. Rev. A* **1984**, *29*, 2054.

Table 1. Composition of Bare Latex Mixtures and the Corresponding Parameters κR_C, U_0 (eq 19) and I_0 (eq 15) for the Four Mixtures of Bare Latex Particles with Hydrodynamic Radius R_h = 330 Å (SANS-determined Radius R_C = 282.5 Å)[a]

mixture	latex (%)	H_2O (%)	D_2O (%)	κR_C	U_0	I_0 (cm^{-1})
1%	1.0	5.1	93.9	9.12	177.15	2450
5%	4.9	25.2	69.9	9.30	171.20	5761
10%	10.0	51.0	39.0	9.53	163.72	2051
15%	14.8	75.6	9.6	9.73	157.63	343

[a] The percentages shown represent weight fractions.

mixtures makes this quantity large, typically ≈10, and very weakly dependent on n_C. For such large values, the effective potential between the colloidal particles is given by the nonlinear solution of the Poisson−Boltzmann equation as[11]:

$$\beta V_{elec}(r) = \begin{cases} \infty, & r < 2R_C; \\ U_0 \ln\{1 + \exp[-\kappa(r - 2R_C)]\}, & r > 2R_C, \end{cases} \quad (18)$$

where

$$U_0 = \frac{(Ze)^2}{8\pi k_B T \epsilon_0 \epsilon_r R_C (1 + \kappa R_C)^2} \quad (19)$$

The values of U_0 for the four mixtures are shown in Table 1.

To determine the structure factor resulting from this interaction potential, a numerical solution of the Ornstein−Zernike equation with the Rogers−Young closure[19] was performed as a function of colloid concentration. The Rogers−Young closure is "thermodynamically consistent",[19,20,27] thus yielding a very accurate prediction of the structure factor that can be considered exact. Consequently, deviations from the measured structure factor can be attributed to deviations from the assumed form of the pair potential, all other factors being equal.

3.5. Gelatin-Coated Particles Interaction Potential. The surface potential of gelatin-coated R_h = 330 Å particles was measured to be $\psi_0 = -27$ mV, corresponding to an effective particle charge of $Z = 431$. For simplicity, we locate this charge at the surface of the colloid, ignoring both the complexity of the actual charge distribution in the corona and the interpretation of the measured electrophoretic mobility.

For separation distances less than twice the gelatin corona length L, the effective interaction between coated particles also includes a steric repulsion resulting from the concentration of gelatin between the approaching particles. In previous work, Kamiyama and Israelachvili[12] demonstrated that the Alexander−de Gennes[13,14] potential described their surface forces measurements of gelatin adsorbed to macroscopic mica cylinders at similar solution conditions. Further, the gelatin layers were stable and could be considered "anchored" for purposes of interpreting the experiment. Thus, we follow the same approach here and we show that the above-mentioned potential can also describe the effective interaction, suitably modified for the spherical colloidal geometry, for our system.

Our starting point is the Alexander−de Gennes expression[13,14] for the repulsive pressure P between two brush-bearing planar surfaces, each coated with a brush layer of thickness L, expressed as a function of the interplate separation D:

$$P(D) = \begin{cases} (k_B T/s^3)\left[\left(\frac{2L}{D}\right)^{9/4} - \left(\frac{D}{2L}\right)^{3/4}\right], & D \le 2L; \\ 0, & D > 2L, \end{cases} \quad (20)$$

where s is the mean distance between two polymeric molecules on the surface. Using the thermodynamic relation $P(D) = -\partial\Phi_{FP}(D)/\partial D$, where $\Phi_{FP}(D)$ is the free energy per unit area of two flat plates separated by a distance D, we obtain the latter quantity as:

$$\beta\Phi_{FP}(D) = \frac{8L}{35s^3}\left[7\left(\frac{2L}{D}\right)^{5/4} + 5\left(\frac{D}{2L}\right)^{7/4} - 12\right] \quad (21)$$

where $\beta = (k_B T)^{-1}$. The expression above holds for $D \le 2L$; for larger separations, $\beta\Phi_{FP}(D)$ vanishes.

The effective pair potential between two spherical rigid particles of radius R_C, each covered with a corona of thickness L, can be obtained from the quantity $\beta\Phi_{FP}$ by use of the Derjaguin approximation.[11] In particular, if we call r the distance between the centers of the particles and $h = r - 2R_C$ the distance of closest approach between the surfaces, the steric repulsion $\beta V_{st}(h)$ is given by the expression[11]:

$$\beta V_{st}(h) = \pi R_C \int_h^{2L} \beta\Phi_{FP}(D)dD, \ (0 \le h \le 2L) \quad (22)$$

For $h \ge 2L$, $\beta V_{st}(h)$ vanishes, whereas for $r < 2R_C$ we have the usual hard-sphere repulsion. Performing the integral we finally obtain:

$$\beta V_{st}(r) = \begin{cases} \infty, & r < 2R_C; \\ f(y), & 2R_C < r \le 2(R_C + L); \\ 0, & 2(R_C + L) < r, \end{cases} \quad (23)$$

where $y = (r - 2R_C)/(2L)$ and

$$f(y) = \frac{16\pi R_C L^2}{35s^3}\left[28(y^{-1/4} - 1) + \frac{20}{11}(1 - y^{11/4}) + 12(y - 1)\right] \quad (24)$$

As with the previous work, we assume the steric and electrostatic repulsions can be added linearly. Note that such a clear separation between charge and compression effects is thought possible because of the strong screening of the additional charges of the polyampholyte by the ions of the added salt. We obtain the total pair potential between gelatin-coated particles $\beta V_{tot}(r)$ as:

$$\beta V_{tot}(r) = \beta V_{elec}(r) + \beta V_{st}(r) \quad (25)$$

with $\beta V_{elec}(r)$ and $\beta V_{st}(r)$ given by eqs 18 and 23 respectively. The only parameter that still has to be determined is the intermolecular distance s on the surface. To fix the value of s, we follow the procedure of Kamiyama and Israelachvili[12]: from the measured mass of adsorbed gelatin, gelatin molecular weight, and measured particle size, we determine the average number of gelatin molecules adsorbed N_{ads} adsorbed on the latex particle of surface area A. Then, the quantity s is given by the formula $s = \sqrt{A/N_{ads}}$. The results are summarized in Table 2, together with the solvent compositions for the two different mixtures of gelatin-coated particles we considered.

Using this composite pair potential, once more with no free fit parameters, we obtain predictions for the structure factor of gelatin-coated colloidal particles from numerical

Table 2. Composition of Mixtures Containing both R_C = 282.5 Å Latex and Gelatin[a]

mixture	latex (%)	gelatin (%)	H_2O (%)	D_2O (%)	net gelatin (mg/m^2)	adsorbed gelatin (mg/m^2)	*s* (nm)
I	9.8	0.1	83.3	6.8	0.12	0.07	48.90
II	9.8	1.0	82.4	6.8	1.0	0.5	18.25

[a] The percentages shown correspond to weight fractions.

solutions of the Ornstein−Zernike−Rogers−Young (OZ-RY) equation for direct comparison with the measured SANS scattering spectra.

4. Results and Discussion

In this section, we proceed by first determining the particle form factor, which yields R_C, from SANS measurements of the dilute scattering from bare latex particles. Then, we show results of contrast matching experiments on dilute gelatin-coated latex to determine the extent of the gelatin corona, i.e., the parameter *L*. Then, using the known scattering length densities and solution compositions we compare a priori predictions for the SANS scattering for concentrated charge-stabilized dispersions to show the validity of the proposed electrostatic potential model. We then extend the analysis to gelatin-coated latex, where we use the known gelatin adsorption isotherms to again make a priori predictions for the scattering spectra of concentrated dispersions with varying gelatin coverage. Finally, these results are extended to a second latex of slightly larger radius with a fixed gelatin coverage, studied as a function of total gelatin/colloid concentration.

Results have been published[7] for the dilute limiting scattering from these latex particles with and without adsorbed gelatin. These results are briefly reproduced and discussed below as a prelude to the analysis of the concentrated latex dispersions.

This procedure outlined above is performed at 1% weight latex concentration; the solvent composition is given in Table 1. The fits are shown in Figure 1, yielding R_C = 282.5 Å for the latex-particle radius. As shown, multiple minima and maxima can be fit successfully by a spherical, homogeneous sphere model. This value compares well with the hydrodynamic radius as determined from dynamic light scattering (330 ± 30 Å), which is usually observed to be slightly greater than SANS radii for most polymer laticies. Independent analysis using a polydisperse form factor shows that the value of polydispersity is on the order of 6%, in agreement with the DLS measurements and thus negligible for the subsequent analysis to be shown below. Because the sample−detector distance L_2 affects the instrument resolution function, we show independent results obtained for two different detector distances.

The scattering profiles from dilute solutions of acrylic latex with adsorbed gelatin (equilibrated with 0.1% and 0.2% weight gelatin solutions) are shown in Figure 2. Because the scattering length density of the solvent is adjusted to nearly match the latex core, the absolute scattering intensity is nearly 3 orders of magnitude smaller than that for the bare latex, necessitating a much longer experiment. As mentioned above, the fits are performed with only the gelatin corona thickness as an adjustable parameter, which seems to be justifiable given the quality of the fits. As noted previously, we use the measured adsorbed amount, determined by fluorimetry and a solution depletion method (as described in ref 7), along with the assumption of a uniform corona composition. Our measurements do not extend to low enough scattering vectors to yield accurate measurements of the adsorbed amounts by the surface Guinier method, and we neglect

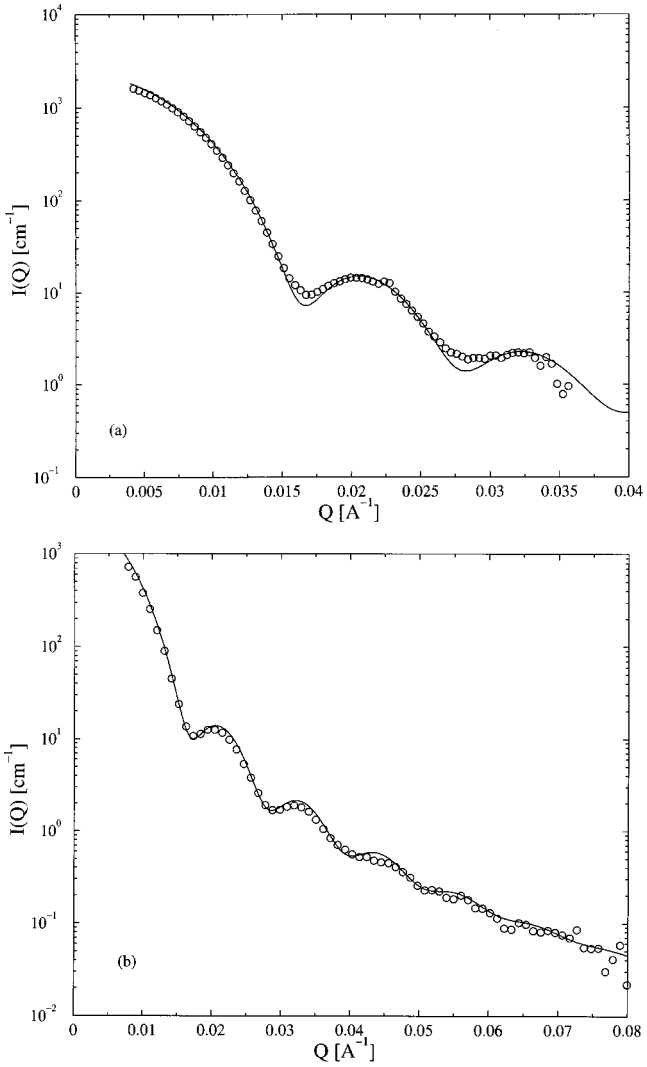

Figure 1. SANS measurements of the bare particle form factor for 330 Å acrylic latex at 1% weight latex, where interparticle correlations can be ignored. The lines are theoretical fits to the data according to eq 7, used to extract the particle radii. Results for two different values of the sample−detector distance L_2 are shown: (a) L_2 = 13 m; (b) L_2 = 5 m.

any contributions caused by fluctuations, as discussed in ref 8. The uncertainty in the corona thickness is determined by a visible worsening of the theoretical fits of the data. As can be seen from Figure 2, good agreement is achieved within the core−shell model. Both fits yield the same net coated particle size, R_M = 390 ± 20 Å. Hence, the gelatin corona has thickness L = 107.5 Å.

We solved the OZ-RY equation[19] with the pair potential parameters shown in Table 1 to obtain the structure factor $S(Q)$ and the total scattering intensity according to eq 14 for the concentrated, electrostatically stabilized latex dispersions with composition given in Table 1. The theoretical results are shown in comparison with the experimental data in Figure 3. Because the value of the prefactor I_0 (see eq 15) is also fixed, our approach contains no free fit parameters. Excellent agreement between

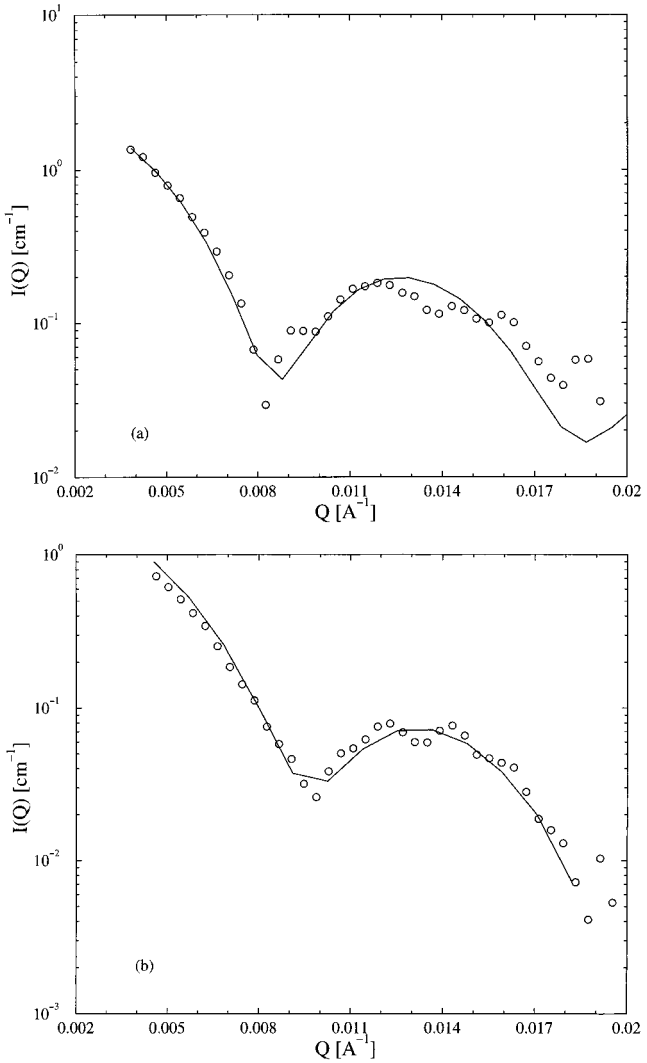

Figure 2. SANS-measured scattering from the gelatin corona on 330 Å acrylic latex: (a) nearly contrast matched in equilibrium with 0.1% weight gelatin; (b) contrast matched in equilibrium with 0.2% weight gelatin. The lines are fits according to eq 10 with $R_C = 282.5$ Å and $R_M = 390$ Å; The latex concentration was 0.36 wt % for both samples.

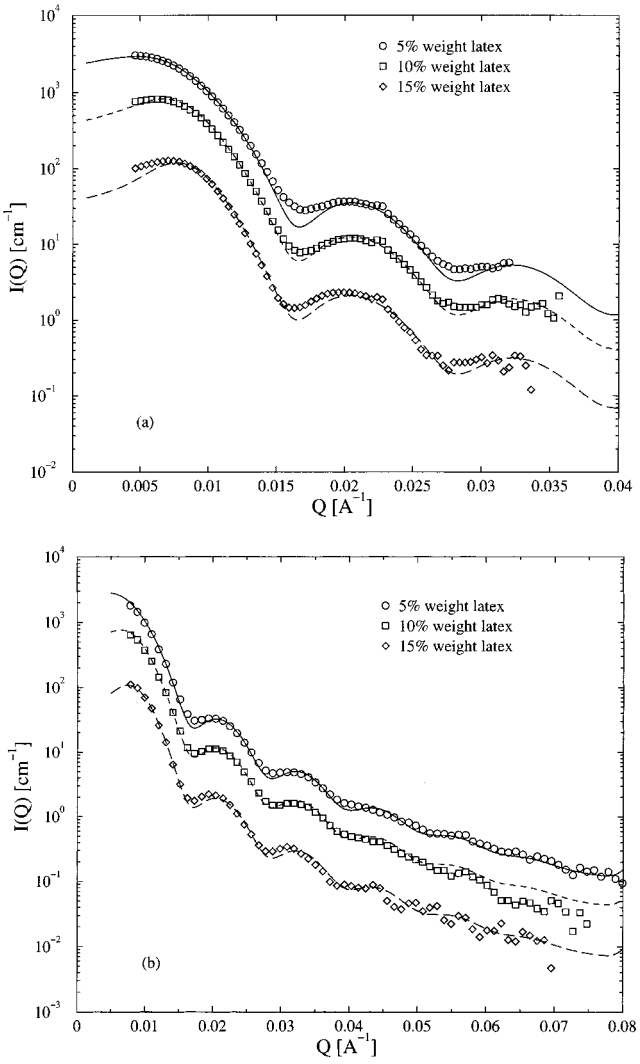

Figure 3. SANS-measured scattering from bare latex solutions (points) and the corresponding to theoretical results (lines). Data from two different values of the sample−detector distance L_2 are shown: (a) $L_2 = 13$ m; (b) $L_2 = 5$ m.

theory and SANS data is obtained by using the electrostatic pair potential, eq 18, for the bare latex particles. Deviations are seen for the highest concentration at the longest detector distance and at lowest scattering vector, just next to the beam stop. This may be a consequence of finite polydispersity, but is equally likely to be a consequence of combined detector smearing and poor statistics in circular averaging over a limited number of detection cells.

Because of the high concentration of salt, the electrostatic potential is strongly screened and, therefore, the hard core plays the most important role. A truly rigorous test of the potential would also include variation in the added salt concentration and the colloid concentration, but this is beyond the scope of this study. In fact, it would also be possible to describe theoretically the present SANS data by performing a mapping of the electrostatic potential to an effective hard sphere system.[27]

For the gelatin-coated particles, using the composite interaction potential of steric plus electrostatic repulsion and solving the OZ-RY equation yields the theoretical results for the total scattering intensities shown in Figure 4. The solution properties are listed in Table 2. The good quality of the agreement between theory and experiment demonstrates the validity of this effective pair potential. In Figure 5 we also show the bare structure factors for the two solutions. Note that the average density of colloidal particles is the same for both solutions; they only differ in the amount of gelatin adsorbed and thus on the steepness of the steric repulsive potential. This is manifested in the shape of $S(Q)$ for the higher gelatin concentration, which displays more structure at higher total adsorbed gelatin. In this analysis we assume that the layer thickness is constant and that only the prefactor of the steric potential changes. Moreover, the dispersion with higher adsorbed amount has its peak at a slightly smaller Q-value than the dispersion with the lower adsorbed amount, pointing to the fact that particles with a dense gelatin coating are more repulsive and thus separate further on average.

The relative contributions of the electrostatic and steric repulsions to the stability of the gelatin-coated latex are demonstrated in Figure 6a, for 0.1% weight gelatin, and in Figure 6b for 1.0% weight gelatin. In the same figures, we show separately the electrostatic and steric contributions. As can be seen, for the lower gelatin concentration, the steric contribution is negligible compared with the electrostatic one, whereas for the higher concentration the two contributions are similar. The additional steric repulsion between the adsorbed gelatin layers provides

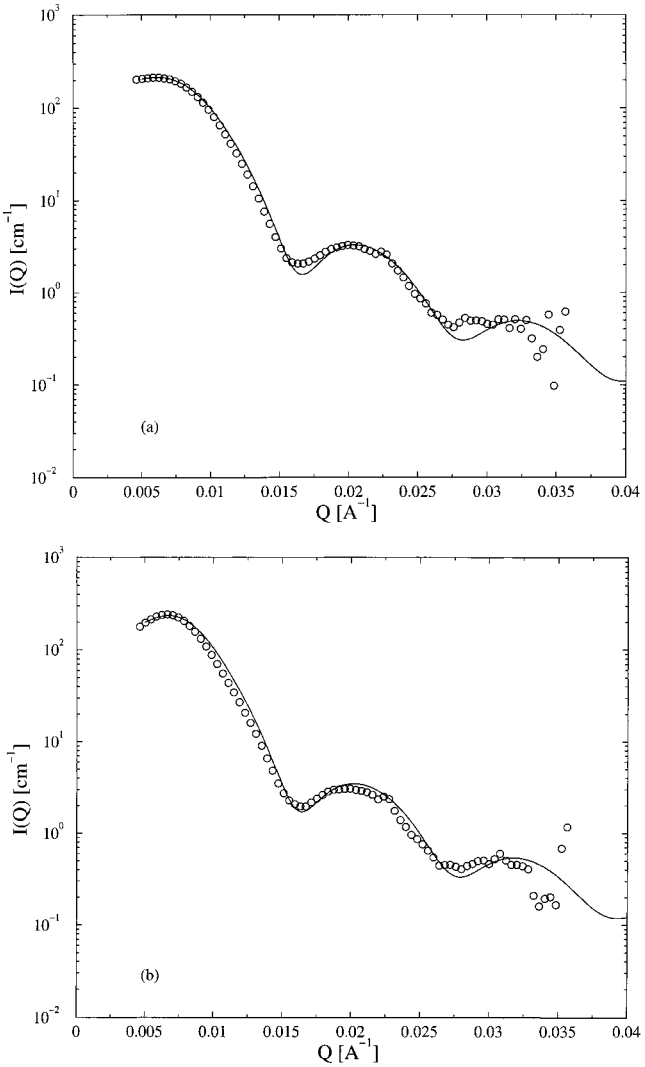

Figure 4. SANS-measured scattering from solutions of gelatin-coated latex particles (points) and the corresponding to theoretical results (lines). (a) Results for mixture I; (b) results for mixture II (see Table 2).

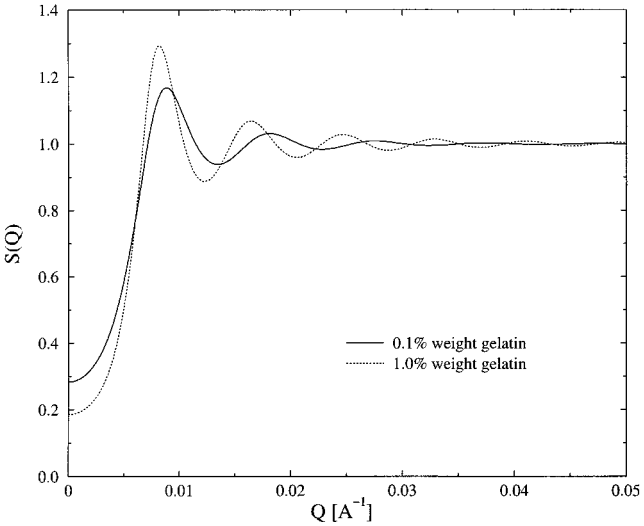

Figure 5. The "bare" structure factors for the 0.1% weight gelatin and the 1.0% weight gelatin solutions of coated latex particles, as calculated from theory, by using the pair potential described in the text.

the major stabilizing effect between the colloidal particles and causes the main peak in the structure factor to shift

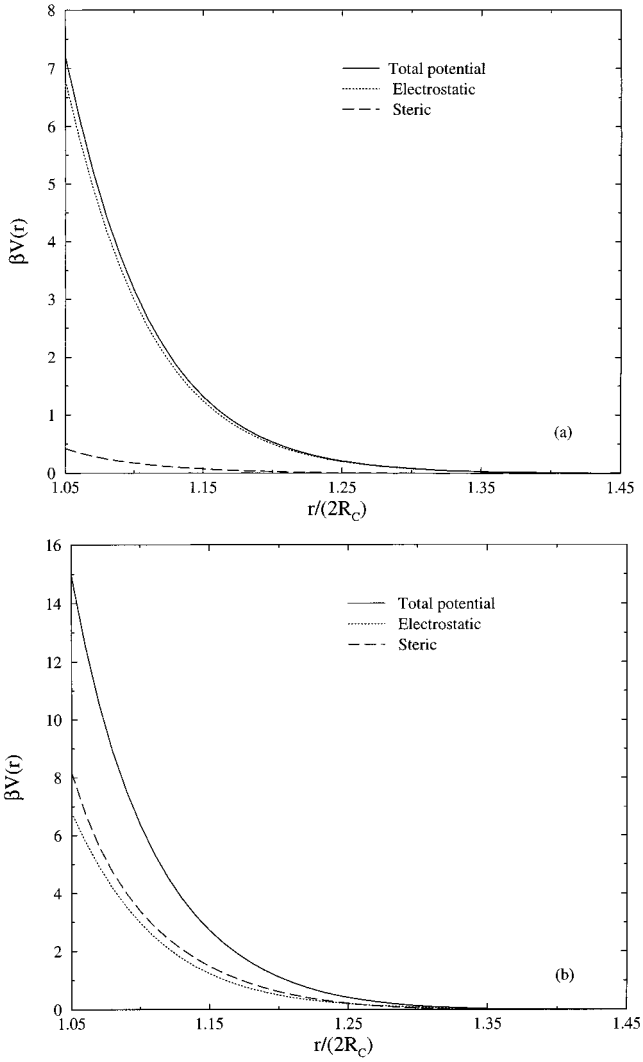

Figure 6. The effective interaction between gelatin-coated colloids, as given by eq 25 in the text: (a) 0.1% weight adsorbed gelatin and (b) 1.0% weight adsorbed gelatin. The electrostatic and steric contributions are also shown separately for both cases.

to higher Q-values, as shown in Figure 5. Apart from these quantitative remarks, we can also see from Figure 6 that, because of the high salt concentration, the effective interaction between the colloidal particles is short-ranged, which agrees with previous results by Kamiyama and Israelachvili on slightly curved cylindrical mica surfaces.[12]

To further investigate the validity of the above-mentioned effective pair potential for gelatin-coated colloids, we performed the same theoretical procedure for another set of SANS data, taken this time on mixtures of fully coated latex colloidal particles having a larger radius, $R_C = 400$ Å, at four different colloidal concentrations. The ratio of adsorbed gelatin to colloid is held fixed in this series of experiments. We denote these mixtures III−VI and summarized their properties in Table 3. The parameter s has been calculated as described above, and the thickness of the adsorbed gelatin layer L is assumed to be independent of the size of the latex particles, i.e., we take again $L = 107.5$ Å.

Without introducing any fit parameters, again we solve the Rogers−Young closure to calculate the structure factor and compare the theoretical results with the measured scattering intensities. The results for the intensities are shown in Figure 7 and the bare structure factors in Figure 8. Once more, the agreement between theory and experi-

Table 3. Composition of Mixtures Containing Both Latex and Gelatin for the Samples Containing Latex Particles of Radius R_C = 400 Å[a]

mixture	latex (%)	H_2O (%)	D_2O (%)	adsorbed gelatin (mg/m^2)	s (nm)
III	0.3	52.8	46.9	1.5	10.5
IV	1.2	52.4	46.4	1.5	10.5
V	3.9	50.9	45.2	1.5	10.5
VI	8.4	48.5	43.1	1.5	10.5

[a] The percentages shown correspond to weight fractions.

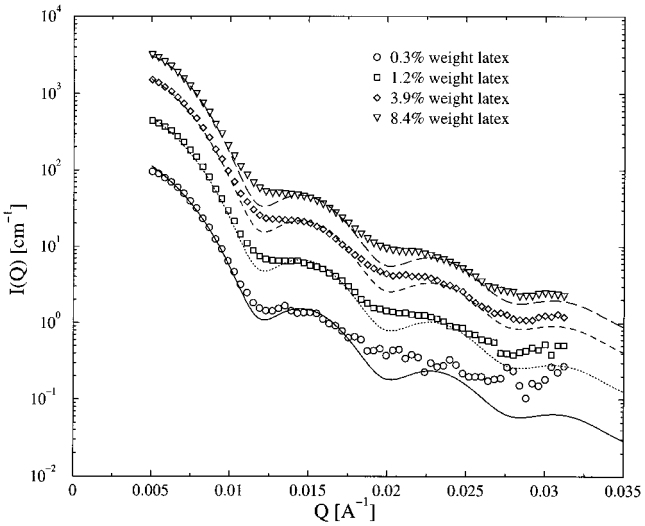

Figure 7. SANS-measured scattering from solutions of gelatin-coated latex particles (points) and the corresponding to theoretical results (lines), for mixtures III−VI (see Table 3).

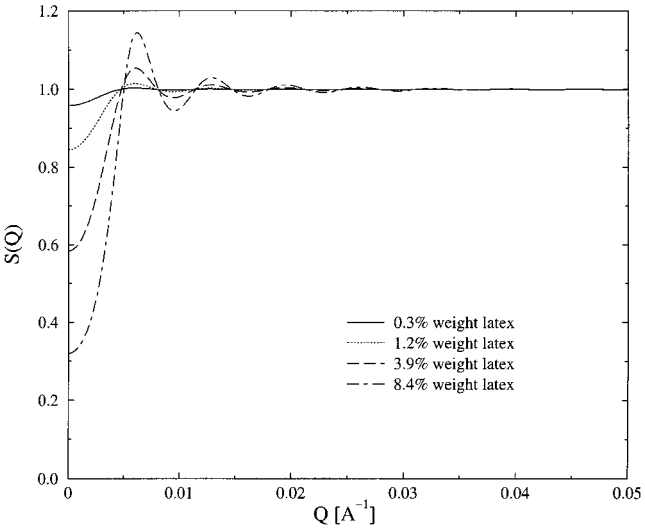

Figure 8. The "bare" structure factors for mixtures III−VI (see Table 3), containing gelatin-coated latex particles of radius R_C = 400 Å.

ment is quantitative, without any fit parameters. Further, the agreement is now across a range of gelatin/colloid complex concentrations, which probe different ranges of the potential. The small discrepancies concerning the minima of the scattering intensities, which are deeper in theory than in experiment, are attributed to the inherent size polydispersity of the latex particles as well as further polydispersity in the interaction potential introduced by the broad molecular weight distribution of the adsorbed gelatin.

5. Conclusions

The adsorption of polyampholytic gelatin onto colloidal acrylic latex of like net charge proceeds with relatively weak adsorption strength (on the order of a few k_BT per molecule) to a saturation of only a few mg/m^2. The adsorption is thought to be primarily driven by charge-induced electrostatic polarization.[7,15] The SANS measurements presented here demonstrate that this weakly adsorbed layer provides a significant steric stability. Further, our study shows that the naive superposition of a simple electrostatic repulsion with an equally simple model for polymer steric stabilization is able to accurately represent the interaction static potential between colloidal surfaces with adsorbed gelatin. This conclusion agrees with previous SFA studies; however, here we independently determine all the potential parameters and compare a priori predictions to direct SANS measurements of the colloidal microstructure. Indeed, we have shown that one can predict a priori the liquid structure of concentrated colloidal dispersions resulting from gelatin adsorption by this simple approach.

One technologically important use of gelatin is in providing shear stability during processing, such as in pharmaceutical and color film manufacturing, for example. The experiments and analysis shown here demonstrate that is should be possible to predict a priori the stabilization properties of gelatin from the known adsorbed amounts, gelatin corona thickness, and solution pH and ionic strength. Preliminary studies in our laboratory suggest that gelatin is a very effective stabilizer at these solution physicochemical conditions against shear-induced aggregation, qualitatively confirming the strong steric repulsion afforded by the relatively minor gelatin layer. Despite these successes, the accuracy of this simple, potential approach to modeling the complex interactions of weakly adsorbed polyampholyte layers is expected to break down when dynamical properties are considered. In particular, dispersion rheology and dense dispersion diffusion may be expected to be sensitive to the details of the adsorbed layer structure and its dynamics, in contrast to the static SANS measurements studied here. Consequently, further work is warranted to examine the details of the dynamical colloidal interactions imparted by adsorbed polyampholytes, as well as other interactions, such as bridging, that may play a role at solution physicochemical conditions other than those studied here.

Acknowledgment. We thank the Alexander von Humboldt-Stiftung, the U.S. National Academy of Sciences and the DAAK (Deutsch-Amerikanisches Akademisches Konzil) for financial support within a GARN project for travel to facilitate this collaboration. This material is based on activities supported by the National Science Foundation under agreement DMR-9122444. We acknowledge the support of the National Institute of Standards and Technology, U.S. Department of Commerce, in providing the facilities for the SANS experiments. We also acknowledge Dr. Ravi Sharma of Eastman Kodak Company for useful discussions and providing the gelatin and colloids used in this study. In addition, N.J.W. and K.A.V. thank Dr. James Brady of Hercules, Inc. for use of equipment for electrophoretic mobility measurements, and Dr. David Locker of Eastman Kodak and the Delaware Research Partnership for financial support.

LA991142D